

## Performance of PdAu/Al<sub>2</sub>O<sub>3</sub> egg-shell catalyst with isolated Pd<sub>1</sub> sites for selective hydrogenation of acetylene

Igor S. Mashkovsky,<sup>\*a</sup> Nadezhda S. Smirnova,<sup>a</sup> Pavel V. Markov,<sup>a</sup> Galina N. Baeva,<sup>a</sup> Anastasia E. Vaulina,<sup>a,b</sup> Dmitry P. Melnikov<sup>a,c</sup> and Alexander Yu. Stakheev<sup>a</sup>

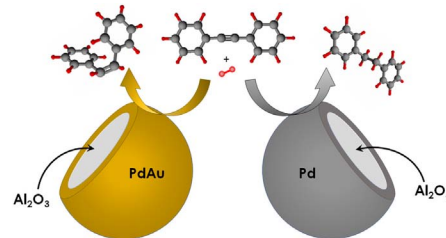
<sup>a</sup> N. D. Zelinsky Institute of Organic Chemistry, Russian Academy of Sciences, 119991 Moscow, Russian Federation. E-mail: [im@ioc.ac.ru](mailto:im@ioc.ac.ru)

<sup>b</sup> D. I. Mendeleev University of Chemical Technology of Russia, 125047 Moscow, Russian Federation

<sup>c</sup> National University of Oil and Gas 'Gubkin University', 119991 Moscow, Russian Federation

DOI: 10.1016/j.mencom.2024.09.030

A herein proposed PdAu/Al<sub>2</sub>O<sub>3</sub> egg-shell catalyst for selective acetylene hydrogenation combines two factors to provide perfect performance: isolation of Pd<sub>1</sub> active sites by Au and an egg-shell distribution of the active phase across the catalyst pellets. The PdAu/Al<sub>2</sub>O<sub>3</sub> catalyst exhibits high acetylene hydrogenation activity at the level of Pd-catalysts and high intrinsic ethylene selectivity of Au-catalysts.



**Keywords:** egg-shell catalyst, palladium, gold, acetylene, ethylene, hydrogenation, single-atom alloy catalyst, selectivity.

Ethylene is the most abundant chemical in the petrochemical industry.<sup>1,2</sup> Produced by steam cracking, ethylene cuts contain up to 2.0 vol% of acetylene. Meanwhile, even traces of acetylene deteriorate the performance of the Ziegler–Natta catalysts. Polymer-grade ethylene streams have to contain acetylene at ppm and even ppb levels. Selective semi-hydrogenation of acetylene on supported palladium catalysts is a common method for removal of alkyne impurities from ethylene cuts.<sup>3,4</sup> Palladium exhibits high activity in the hydrogenation of acetylene, but low selectivity to ethylene. Developing new efficient catalysts for ethylene production with high activity, selectivity and stability is a challenging task in both academia and industry.

One of the promising methods to improve ethylene selectivity is to decrease active sites of the palladium to the size of a single atom by dissolving them in the less reactive host metal to obtain single-atom alloy (SAA) catalyst.<sup>5–7</sup> To improve alkene selectivity, transition metals can be used.<sup>8–16</sup> Group 11 metals are among effective promoters for SAA catalysts as they are preferentially located on the surface of bimetallic particles due to their lower surface energy.<sup>3</sup> Moreover, certain group 11 metals (*e.g.*, gold) exhibit an intrinsic ultra-high ethylene selectivity of approximately 100%, however their activity is very low.<sup>17,18</sup> The addition of ultra-low amounts of palladium with subsequent formation of PdAu alloy may be a promising way to increase the activity of gold catalysts in acetylene hydrogenation without altering the high alkene selectivity.<sup>19</sup>

Modern industrial catalysts for acetylene hydrogenation have an egg-shell structure, meaning that the active phase is distributed only in the thin outer surface layer of the catalyst pellets. Such structure enables a decrease of the active component and minimizes the impact of mass transfer resistance.<sup>20,21</sup> While the properties of PdAu catalysts in selective acetylene hydrogenation are multiply investigated, the number of sources that discuss the performance of a PdAu egg-shell catalysts is very scarce.<sup>13,22–26</sup>

In this work we obtain a novel bimetallic egg-shell PdAu/Al<sub>2</sub>O<sub>3</sub> catalyst (Au/Pd molar ratio of 5:1) with Pd<sub>1</sub> isolated active sites. Previously, a PdAg catalysts with similar structure demonstrated promising performance in this reaction.<sup>27,28</sup> Monometallic Pd and Au catalysts were used as references.

The structure of the synthesized egg-shell catalyst was characterized by TEM (Figure 1). The metal nanoparticles are spherical in shape with an average size of approximately 6 nm for Pd/Al<sub>2</sub>O<sub>3</sub>, 15 nm for PdAu/Al<sub>2</sub>O<sub>3</sub> and 12 nm for Au/Al<sub>2</sub>O<sub>3</sub> samples. The lattice plane distance of the PdAu particle is estimated as 2.3 Å, which is between the distances of Pd (2.23 Å) and Au (2.34 Å) metals both of (111) facets, indicating the formation of PdAu alloy nanoparticles.<sup>29,30</sup>

Metal distribution plays an important role in the outcome of hydrogenation of acetylene using industrially relevant egg-shell catalysts. Note that activity and selectivity can be significantly affected by pore diffusion depending on the thickness of the active shell. To determine the metal distribution, electron probe microanalysis (EPMA) was performed (see Online Supplementary Materials, Figure S1). A homogeneous distribution for Pd and Au was obtained for the PdAu/Al<sub>2</sub>O<sub>3</sub> catalyst. The thickness of the active shell was defined as the depth of Pd and was approximately

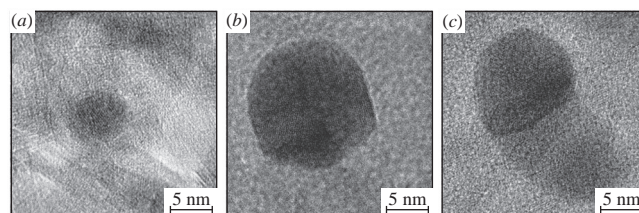


**Figure 1** Typical TEM images of (a) Pd/Al<sub>2</sub>O<sub>3</sub>, (b) PdAu/Al<sub>2</sub>O<sub>3</sub> and (c) Au/Al<sub>2</sub>O<sub>3</sub> egg-shell catalysts.

0.21–0.29 mm for both catalysts, which is close to industrial application.<sup>21</sup>

DRIFT spectra of adsorbed CO in the region of 2250–1850 cm<sup>−1</sup> are presented on Figure 2. The monometallic palladium catalyst (curve 1) shows a symmetric band centered at ~2076 cm<sup>−1</sup> and a broad asymmetric band in the range of 2000–1850 cm<sup>−1</sup>. The peak with maximum at 2076 cm<sup>−1</sup> is ascribed to CO linearly adsorbed on palladium atoms (corners, edges or surface defects).<sup>31,32</sup> The band below 2000 cm<sup>−1</sup> can be attributed to multibonded CO adsorbed on large planes of palladium nanoparticles. It is known that the bands at 2000–1950 cm<sup>−1</sup> can be assigned to compressed-bridged CO, whereas bands at 1950–1900 cm<sup>−1</sup> are attributed to isolated-bridged CO on Pd facets. The small shoulder at 1900–1850 cm<sup>−1</sup> corresponds to multiply bonded CO species on hollow Pd sites of (111) facets.

In contrast to Pd/Al<sub>2</sub>O<sub>3</sub>, monometallic Au/Al<sub>2</sub>O<sub>3</sub> exhibits a single peak with maximum at ~2105 cm<sup>−1</sup> (see Figure 2, curve 2), which corresponds to CO linearly adsorbed onto the low coordinated sites of metallic Au particles (corners, edges, etc.).<sup>33–35</sup> The complete absence of bands below 2000 cm<sup>−1</sup> is characteristic for monometallic gold particles.<sup>34,36,37</sup> A broad band with very low intensity at ~2200–2150 cm<sup>−1</sup> is attributed to R-branch of CO in gaseous state.

DRIFT CO spectrum of bimetallic Pd–Au/Al<sub>2</sub>O<sub>3</sub> sample (see Figure 2, curve 3) significantly differs from the summation of monometallic palladium and gold spectra. The sharp peak centered at 2110 cm<sup>−1</sup> is ascribed to linearly adsorbed CO on the defects of Au<sup>0</sup> nanoparticles, whereas the band with maximum at ~2076 cm<sup>−1</sup> may contain several components.<sup>34</sup> The main component centered at ~2076 cm<sup>−1</sup> is also ascribed to linearly bonded CO on low-coordinated Pd atoms. According to the decomposition of this band it is possible that minor components with maxima in 2060–2040 cm<sup>−1</sup> may be related to linear CO adsorbed on Pd atoms on the facets.<sup>34</sup> The addition of Au to Pd catalyst leads to almost complete disappearance of bands below 2000 cm<sup>−1</sup>, leaving only a small feature centered at 1967 cm<sup>−1</sup>. Since the formation of bridge-bonded CO on monometallic gold is unlikely, this observation suggests that palladium dissolves in gold forming alloy particles on the surface of the bimetallic Pd–Au egg-shell catalyst. As demonstrated previously, the absorption band at 1967 cm<sup>−1</sup> can be attributed to bridged-bonded CO on Pd–Au atoms and/or Pd–Pd dimers, predominantly located at the edge-edge sites.<sup>34</sup> Since the extinction coefficient for bridged-bonded CO band is ~20–25 times higher than for linear CO,<sup>38,39</sup> it can be assumed that the degree of Pd dilution by Au is sufficiently high.<sup>40</sup> Presumably, the obtained bimetallic PdAu surface alloy approaches the

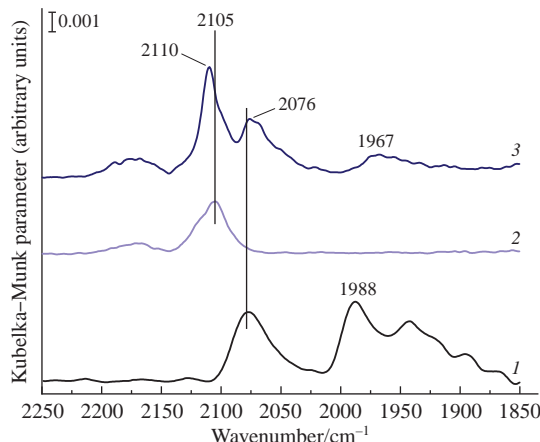


**Figure 2** DRIFT spectra of adsorbed CO for freshly reduced catalysts: (1) Pd/Al<sub>2</sub>O<sub>3</sub>, (2) Au/Al<sub>2</sub>O<sub>3</sub> and (3) Pd–Au/Al<sub>2</sub>O<sub>3</sub>.

‘single-atom’ structure, where palladium atoms are isolated from each other by atoms of less reactive host element.<sup>7</sup>

The performance of Pd/Al<sub>2</sub>O<sub>3</sub>, Au/Al<sub>2</sub>O<sub>3</sub>, and PdAu/Al<sub>2</sub>O<sub>3</sub> egg-shell catalysts was evaluated in the selective acetylene hydrogenation in excess of ethylene (Figure 3). The catalyst loading was the same (0.250 g) in each experiment for better comparison. Note that the addition of large amounts of gold did not significantly reduce the activity of the catalyst. Both Pd/Al<sub>2</sub>O<sub>3</sub> and PdAu/Al<sub>2</sub>O<sub>3</sub> catalysts have similar activities under ~30–70 °C and reach 100% acetylene conversion at 90 and 115 °C, respectively [see Figure 3(a)]. The Au/Al<sub>2</sub>O<sub>3</sub> monometallic sample exhibits an extremely low activity in acetylene hydrogenation, with a C<sub>2</sub>H<sub>2</sub> conversion below 5% within the temperature range of 30 to 120 °C. Therefore, selectivity to ethylene of Au-catalyst could not be determined due to a large instrumental error. The result obtained for the Au-catalyst is consistent with previously reported data which suggest that increasing the temperature to 150–300 °C is necessary to enhance its activity.<sup>18,41</sup>

The ethylene selectivity for Pd/Al<sub>2</sub>O<sub>3</sub> catalyst remains high (~96%) in the region of low acetylene conversions (<50%) [see Figure 3(b)]. With the increase of acetylene conversion to 80% the selectivity of ethylene decreases rapidly to 20% and reaches ~98% at acetylene conversion of 100%. The negative ethylene selectivity means that some of initial ethylene in the feedstock is converted to ethane.<sup>33</sup> In the case of PdAu catalyst, the selectivity to ethylene is noticeably higher (86%) compared to monometallic Pd (~21%) at acetylene conversion of ~77–80%. Furthermore, for the PdAu/Al<sub>2</sub>O<sub>3</sub> catalyst, selectivity to ethylene decreases more slowly with increasing acetylene conversion compared to Pd/Al<sub>2</sub>O<sub>3</sub> catalyst. As was shown by DRIFT CO spectroscopy, the addition of gold to palladium catalyst leads to bimetallic PdAu alloy formation with a significant predominance of isolated palladium atoms on the surface. Despite the relatively low Au/Pd molar ratio (5 : 1), DRIFT spectrum of Pd–Au sample strongly resembles the spectroscopic data,<sup>34</sup> where the molar Au/Pd ratio was close to 20 : 1. This can be explained by the tendency of gold to preferentially locate on the surface due to its lower surface energy than that of Pd. DRIFTS CO data confirmed the absence of large multiaatomic Pd<sub>n</sub> (where  $n \geq 2$ ) ensembles with negligible amounts of ‘bridged’ Pd<sub>2</sub> sites. Therefore, it can be assumed that increase in C<sub>2</sub>H<sub>4</sub> selectivity in the case of the

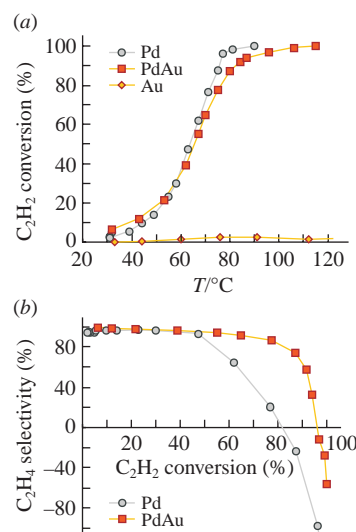


**Figure 3** Performance of Pd–Au/Al<sub>2</sub>O<sub>3</sub>, Pd/Al<sub>2</sub>O<sub>3</sub> and Au/Al<sub>2</sub>O<sub>3</sub> egg-shell catalysts in acetylene hydrogenation: (a) C<sub>2</sub>H<sub>2</sub> conversion vs. the reaction temperature and (b) C<sub>2</sub>H<sub>4</sub> selectivity vs. C<sub>2</sub>H<sub>2</sub> conversion;  $m_{\text{cat}} = 0.250$  g,  $H_2/C_2H_2 = 5$ .

PdAu egg-shell catalyst may result from the formation of a structure close to a ‘single-atom’ alloy.

In summary, a novel bimetallic egg-shell type PdAu/Al<sub>2</sub>O<sub>3</sub> catalyst was synthesized. The sample was obtained by convenient technique of consecutive incipient wetness impregnation with palladium and gold aqueous solutions, which made it possible to deposit the gold component in the outer shell of Al<sub>2</sub>O<sub>3</sub> sphere in close proximity with the first metal. The formation of PdAu solid solution with a surface structure close to ‘single-atom’ alloy was confirmed by DRIFT spectroscopy of adsorbed CO. In the gas-phase selective acetylene hydrogenation PdAu/Al<sub>2</sub>O<sub>3</sub> catalyst exhibited excellent ethylene selectivity without any noticeable decrease in activity. Thus, this approach can be effective for obtaining egg-shell palladium–gold acetylene hydrogenation catalysts with improved ethylene selectivity. The data obtained may provide valuable information for the rational design of the Au-based catalysts.

This work was supported by the Russian Science Foundation (grant no. 23-13-00301; <https://rscf.ru/en/project/23-13-00301>). The authors are grateful to A. S. Vishnevich (Gubkin State University) for the transmission electron microscopy study of the catalysts.

#### Online Supplementary Materials

Supplementary data associated with this article can be found in the online version at doi: 10.1016/j.mencom.2024.09.030.

#### References

- 1 K. Xie, K. Xu, M. Liu, X. Song, S. Xu and H. Si, *Mater. Today Catal.*, 2023, **3**, 100029.
- 2 T. D. Shittu and O. B. Ayodele, *Front. Chem. Sci. Eng.*, 2022, **16**, 1031.
- 3 A. Borodzinski and G. C. Bond, *Catal. Rev.*, 2008, **50**, 379.
- 4 B. Rijo, F. Lemos, I. Fonsecab and A. Vilelas, *Chem. Eng. J.*, 2020, **379**, 122390.
- 5 X. Deng, J. Wang, N. Guan and L. Li, *Cell Rep. Phys. Sci.*, 2022, **3**, 101017.
- 6 I. S. Mashkovsky, P. V. Markov, A. V. Rassolov, E. D. Patil and A. Yu. Stakheev, *Russ. Chem. Rev.*, 2023, **92**, RCR5087.
- 7 R. T. Hannagan, G. Giannakakis, M. Flytzani-Stephanopoulos and E. C. H. Sykes, *Catal. Rev.*, 2020, **120**, 12044.
- 8 G. X. Pei, X. Y. Liu, X. Yang, L. Zhang, A. Wang, L. Li, H. Wang, X. Wang and T. Zhang, *ACS Catal.*, 2017, **7**, 1491.
- 9 J. H. Lee, S. K. Kim, I. Y. Ahn, W.-J. Kim and S. H. Moon, *Catal. Commun.*, 2011, **12**, 1251.
- 10 K. Kovnir, M. Armbrüster, D. Teschner, T. V. Venkov, F. C. Jentoft, A. Knop-Gericke, Y. Grin and R. Schlgöl, *Sci. Technol. Adv. Mater.*, 2007, **8**, 420.
- 11 Y. Cao, Z. Sui, Y. Zhu, X. Zhou and D. Chen, *ACS Catal.*, 2017, **7**, 7835.
- 12 D. V. Glyzdova, T. N. Afonasenko, E. V. Khramov, N. N. Leont’eva, M. V. Trenikhin, I. P. Prosvirin, A. V. Bukhtiyarov and D. A. Shlyapin, *Top. Catal.*, 2020, **63**, 139.
- 13 T. V. Choudhary, C. Sivadinarayana, A. K. Datye, D. Kumar and D. W. Goodman, *Catal. Lett.*, 2003, **86**, 1.
- 14 D. Melnikov, V. Stytsenko, E. Savelava, M. Kotelev, V. Lyubimenko, E. Ivanov, A. Glotov and V. Vinokurov, *Catalysts*, 2020, **10**, 624.
- 15 V. D. Stytsenko, D. P. Melnikov, A. P. Glotov and V. A. Vinokurov, *Mol. Catal.*, 2022, **553**, 11275.
- 16 P. V. Markov, N. S. Smirnova, G. N. Baeva, I. S. Mashkovsky, A. V. Bukhtiyarov, I. A. Chetyrin, Ya. V. Zubavichus and A. Yu. Stakheev, *Mendeleev Commun.*, 2023, **33**, 812.
- 17 J. Jia, K. Haraki, J. N. Kondo, K. Domen and K. Tamaru, *J. Phys. Chem. B*, 2000, **104**, 11153.
- 18 A. C. Gluhoi, J. W. Bakker and B. E. Nieuwenhuys, *Catal. Today*, 2010, **154**, 13.
- 19 A. J. McCue, R. T. Baker and J. A. Anderson, *Faraday Discuss.*, 2016, **188**, 499.
- 20 M. T. Ravanchi, S. Sahebdefar, M. R. Fard and H. Moosavi, *Iran. J. Chem. Eng.*, 2021, **18**, 19.
- 21 A. Pachulski, R. Schödel and P. Claus, *Appl. Catal., A*, 2011, **400**, 14.
- 22 C. Ma, Y. Du, J. Feng, Xi. Cao, J. Yang and D. Li, *J. Catal.*, 2014, **317**, 263.
- 23 A. J. McCue and J. A. Anderson, *Front. Chem. Sci. Eng.*, 2015, **9**, 142.
- 24 A. Sarkany, O. Geszti and G. Safran, *Appl. Catal., A*, 2008, **350**, 157.
- 25 H. Miura, M. Terasaka, K. Oki and T. Matsuda, *Surf. Sci. Catal.*, 1993, **75**, 2379.
- 26 S. A. Blankenship, R. W. Voight, J. A. Perkins and J. E. Fried, Jr., *Patent US 6509292 B1*, 2002.
- 27 P. V. Markov, I. S. Mashkovsky, G. N. Baeva, D. P. Melnikov and A. Yu. Stakheev, *Mendeleev Commun.*, 2023, **33**, 836.
- 28 I. S. Mashkovsky, D. P. Melnikov, P. V. Markov, G. N. Baeva, N. S. Smirnova, G. O. Bragina and A. Yu. Stakheev, *Dokl. Chem.*, 2023, **512**, 272 (*Dokl. Ross. Akad. Nauk. Khim., Nauki Mater.*, 2023, **512**, 65).
- 29 F. Han, J. Xia, X. Zhang and Y. Fu, *RSC Adv.*, 2019, **9**, 17812.
- 30 S. H. Wang, Z. L. Xin, X. H. Huang, W. Z. Yu and S. N. Niu, *Phys. Chem. Chem. Phys.*, 2017, **19**, 6164.
- 31 T. Lear, R. Marshall, J. A. Lopez-Sanchez, S. D. Jackson, T. M. Klapötke, M. Bäumer, G. Rupprechter, H.-J. Freund and D. Lennon, *J. Chem. Phys.*, 2005, **123**, 174706.
- 32 S.-K. Kim, C. Kim, J.-H. Lee, J. Kim, H. Lee and S.-H. Moon, *J. Catal.*, 2013, **306**, 146.
- 33 G. X. Pei, X. Y. Liu, A. Wang, L. Li, Y. Huang, T. Zhang, J. W. Lee, B. W. L. Jang and C.-Y. Mou, *New J. Chem.*, 2014, **38**, 2043.
- 34 B. Zhu, G. Thrimurthulu, L. Delannoy, C. Louis, C. Mottet, J. Creuze, B. Legrand and H. Guesmi, *J. Catal.*, 2013, **308**, 272.
- 35 A. Hugon, L. Delannoy, J.-M. Krafft and C. Louis, *J. Phys. Chem. C*, 2010, **114**, 10823.
- 36 S. Zhang, C.-Y. Chen, B. W.-L. Jang and A.-M. Zhu, *Catal. Today*, 2015, **256**, 161.
- 37 J. Liu, J. Shan, F. R. Lucci, S. Cao, E. C. H. Sykes and M. Flytzani-Stephanopoulos, *Catal. Sci. Technol.*, 2017, **7**, 4276.
- 38 M. A. Vannice and S.-Y. Wang, *J. Phys. Chem.*, 1981, **85**, 2543.
- 39 A. J. McCue and J. A. Anderson, *J. Catal.*, 2015, **329**, 538.
- 40 E. K. Hanrieder, A. Jentys and J. A. Lercher, *ACS Catal.*, 2015, **5**, 5776.
- 41 S. Peng, X. Sun, L. Sun, M. Zhang, Y. Zheng, H. Su and C. Qi, *Catal. Lett.*, 2019, **149**, 465.

Received: 11th April 2024; Com. 24/7458